JAM CM Journal of Applied Mathematics and Computational Mechanics 2025, 24(1), 44-55
www.amcm.pcz.pl p-ISSN 2299-9965
DOI: 10.17512/jamcm.2025.1.04 e-ISSN 2353-0588

NUMERICAL SOLUTIONS, STABILITY, AND CHAOS CONTROL OF ATANGANA-BALEANU VARIABLE-ORDER DERIVATIVES IN GLUCOSE-INSULIN DYNAMICS

***Sayed Saber*[1,2], *Safa M. Mirgani*[3]**

[1] *Department of Mathematics, Faculty of Science, Al-Baha University, Saudi Arabia*
[2] *Department of Mathematics and Statistics, Faculty of Science, Beni-Suef University, Egypt*
[3] *Department of Mathematics and Statistics, College of Science, Imam Mohammed Ibn Saud Islamic University, Riyadh, Saudi Arabia*
ssahmed@bu.edu.sa, smmmohamed@imamu.edu.sa

Received: 4 November 2024; Accepted: 18 March 2025

Abstract. Using Atangana-Baleanu fractional variable-order derivatives, this article investigates the impact of memory effects on glucose-insulin dynamics. The uniqueness and boundedness of solutions are established using fixed-point theory. By adjusting the fractional derivative order, different chaotic behaviors can be observed. An Atangana-Baleanu fractional framework is used to analyze Hyers-Ulam stability using the Sumudu transform. Through linear controllers, the Atangana-Baleanu fractional chaotic system can be synchronized, achieving equilibrium. This control mechanism could be beneficial to diabetes management, such as insulin pumps that regulate insulin in real time based on glucose levels. By controlling Atangana-Baleanu fractional order chaos, glucose-insulin regulation could be improved.

MSC 2010: *92D30, 92D25, 92C42, 34C60*
Keywords: *fractional derivatives, nonlinear equations, simulation, numerical results*

1. Introduction

Diabetes, often called a silent epidemic, contributes to the growing burden of noncommunicable diseases. It primarily occurs because of obesity and declining physical activity levels [1]. Since the World Health Organization updated its criteria for diagnosing diabetes mellitus, global prevalence and incidence have surged. Over the past decade, numerous studies have focused on diabetes and its complications. Disease dynamics can be understood and controlled using mathematical models. Nonlinear dynamics are often characterized by chaos, bifurcations, multistability, and other complex behaviors in biological systems [2]. Studies have demonstrated that glucose-insulin interactions display chaotic behavior, as demonstrated by time-series analyses and long-term insulin measurements in ambulatory subjects [3]. Several mathematical models, statistical techniques, and computational methods have been used in these studies. These include glucose-insulin dynamics, diabetes epidemiol-

ogy, and economic costs. Diabetes causes damage to capillary endothelial cells in the retina, mesangial cells in the renal glomerulus, and neurons in peripheral nerves, resulting in retinopathy, nephropathy, and neuropathy [4]. The glucose-insulin dynamics model has evolved from two-dimensional (2D) differential equations [5] to more complex nonlinear three-dimensional (3D) models incorporating β-cells [6]. A recent model based on predator-prey dynamics has highlighted the chaotic behavior of the glucose-insulin regulatory system [7]. A number of studies focus on specific aspects, such as glucose-insulin interactions, computational devices and algorithms, the glycemic index, and the economic burden [8]. Fractional calculus provides a framework for modeling systems with memory and hereditary properties, which are essential for accurately capturing the dynamics of glucose and insulin regulation in biological systems (e.g., [9–15]). Advanced numerical methods, including fixed--point theory and Sumudu transforms, improve computational efficiency and stability in solving nonlinear chaotic systems [16–23]. These methods are particularly suited to biological applications where memory-dependent processes influence system dynamics.

In recent years, fractional calculus has emerged as a powerful tool for modeling systems with long-range memory effects and non-local interactions. A diabetes study using it revealed improvements in glucose-insulin dynamics models, providing further insights into disease progression and treatment options. A number of fractional derivative operators, including the Atangana-Baleanu, Atangana-Baleanu--Caputo, and Riemann-Liouville derivatives, have been employed in these models, each having its own benefits based on the kernel functions they incorporate [24].

We investigate glucose-insulin dynamics using fractional Atangana-Baleanu derivatives, which incorporate memory effects via Mittag-Leffler functions. This approach enables the analysis of chaotic behavior, stability, and synchronization in variable-order systems. Fixed-point theory ensures solution existence, while the Sumudu transform and iterative numerical methods improve computational efficiency. Our model advances diabetes management by refining chaos control strategies, particularly for applications like insulin pump therapy. By integrating variable-order derivatives and enhanced stability analysis, this study provides deeper insights into nonlinear disease progression and contributes to personalized treatment strategies in complex biological systems.

2. Model formulation

In [7], Shabestari et al. proposed a model based on the Lotka-Volterra framework [25], incorporating fractional dynamics to analyze the glucose-insulin relationship.

The fractional model is as follows:

$$\begin{aligned}
\dot{\mathtt{x}} &= -\mathtt{b}_1\mathtt{x} + \mathtt{b}_2\mathtt{x}\mathtt{y} + \mathtt{b}_3\mathtt{y}^2 + \mathtt{b}_4\mathtt{y}^3 + \mathtt{b}_5\mathtt{z} + \mathtt{b}_6\mathtt{z}^2 + \mathtt{b}_7\mathtt{z}^3 + \mathtt{b}_{20},\\
\dot{\mathtt{y}} &= -\mathtt{b}_8\mathtt{x}\mathtt{y} - \mathtt{b}_9\mathtt{x}^2 - \mathtt{b}_{10}\mathtt{x}^3 + \mathtt{b}_{11}\mathtt{y}(1-\mathtt{y}) - \mathtt{b}_{12}\mathtt{z} - \mathtt{b}_{13}\mathtt{z}^2 - \mathtt{b}_{14}\mathtt{z}^3 + \mathtt{b}_{21},\\
\dot{\mathtt{z}} &= \mathtt{b}_{15}\mathtt{y} + \mathtt{b}_{16}\mathtt{y}^2 + \mathtt{b}_{17}\mathtt{y}^3 - \mathtt{b}_{18}\mathtt{z} - \mathtt{b}_{19}\mathtt{y}\mathtt{z}.
\end{aligned}$$

with the initial conditions: $\mathtt{x}(0) = \mathtt{x}_0$, $\mathtt{y}(0) = \mathtt{y}_0$, $\mathtt{z}(0) = \mathtt{z}_0$. Here: $\mathtt{x}$ represents glucose concentration, $\mathtt{y}$ represents insulin concentration, and $\mathtt{z}$ represents the population density of β-cells. The parameters $\mathtt{b}_i$ for $i = 1, 2, \ldots, 21$ describe various interaction rates which can be defined in Table 1. The model also incorporates delayed differential and fractional-order systems to represent biological memory dependence, adding flexibility to capture long-term memory, which is critical for accurately modeling complex biological systems [26]. Additionally, the model benefits from fractional-order systems due to the prevalence of fractal characteristics in biological systems [27–31], allowing for realistic predator-prey dynamics and complex behaviors in chaotic systems [32]. Using a fractional approach, the glucose--insulin regulation system is formulated as follows in the sense of the Atangana--Baleanu (AB) operator:

$$\begin{aligned}
{}^{\mathtt{AB}}\mathscr{D}^{\rho}_{0,t}\mathtt{x} &= -\mathtt{b}_1\mathtt{x} + \mathtt{b}_2\mathtt{x}\mathtt{y} + \mathtt{b}_3\mathtt{y}^2 + \mathtt{b}_4\mathtt{y}^3 + \mathtt{b}_5\mathtt{z} + \mathtt{b}_6\mathtt{z}^2 + \mathtt{b}_7\mathtt{z}^3 + \mathtt{b}_{20},\\
{}^{\mathtt{AB}}\mathscr{D}^{\rho}_{0,t}\mathtt{y} &= -\mathtt{b}_8\mathtt{x}\mathtt{y} - \mathtt{b}_9\mathtt{x}^2 - \mathtt{b}_{10}\mathtt{x}^3 + \mathtt{b}_{11}\mathtt{y}(1-\mathtt{y}) - \mathtt{b}_{12}\mathtt{z} - \mathtt{b}_{13}\mathtt{z}^2 - \mathtt{b}_{14}\mathtt{z}^3 + \mathtt{b}_{21},\\
{}^{\mathtt{AB}}\mathscr{D}^{\rho}_{0,t}\mathtt{z} &= \mathtt{b}_{15}\mathtt{y} + \mathtt{b}_{16}\mathtt{y}^2 + \mathtt{b}_{17}\mathtt{y}^3 - \mathtt{b}_{18}\mathtt{z} - \mathtt{b}_{19}\mathtt{y}\mathtt{z}.
\end{aligned} \tag{1}$$

Table 1. Parameter values and definitions from Shabestari et al. [7]

Parameter	Value	Definition
a_1	2.04	Normal decrease in insulin concentration without glucose.
a_2	0.10	Rate of propagation of insulin with glucose.
a_3	1.09	Rising insulin rate with increased glucose concentration.
a_4	–1.08	Rising insulin level rate independently excreted by β-cells.
a_5	0.03	Rising insulin level rate independently excreted by β-cells.
a_6	–0.06	Rising insulin level rate independently excreted by β-cells.
a_7	2.01	Rising insulin level rate independently excreted by β-cells.
a_8	0.22	Insulin effect on glucose.
a_9	–3.84	Rate of decrease in glucose due to insulin excretion.
a_{10}	–1.20	Rate of decrease in glucose due to insulin excretion.
a_{11}	0.30	Normal rising of glucose without insulin.
a_{12}	1.37	Decrease in glucose concentration due to insulin from β-cells.
a_{13}	–0.30	Decrease in glucose concentration due to insulin from β-cells.
a_{14}	0.22	Decrease in glucose concentration due to insulin from β-cells.
a_{15}	0.30	Rate of increase in β-cells due to increased glucose.
a_{16}	–1.35	Rate of increase in β-cells due to increased glucose.
a_{17}	0.50	Rate of increase in β-cells due to increased glucose.
a_{18}	–0.42	Rate of decrease in β-cells due to existing levels.
a_{19}	–0.15	Rate of decrease in β-cells due to existing levels.
a_{20}	–0.19	Represents a constant input/output in the glucose dynamics.
a_{21}	–0.56	Denotes a baseline rate of insulin production.

A time-varying fractional glucose-insulin regulatory system has control AB fractional order as follows:

$$\begin{aligned}
{}^{\mathtt{AB}}\mathscr{D}^{\rho}_{0,t}\mathtt{x} &= -\mathtt{b}_1\mathtt{x}+\mathtt{b}_2\mathtt{x}\mathtt{y}+\mathtt{b}_3\mathtt{y}^2+\mathtt{b}_4\mathtt{y}^3+\mathtt{b}_5\mathtt{z}+\mathtt{b}_6\mathtt{z}^2+\mathtt{b}_7\mathtt{z}^3+\mathtt{b}_{20}-d_1(\mathtt{x}(t)+\mathtt{y}(t)),\\
{}^{\mathtt{AB}}\mathscr{D}^{\rho}_{0,t}\mathtt{y} &= -\mathtt{b}_8\mathtt{x}\mathtt{y}-\mathtt{b}_9\mathtt{x}^2-\mathtt{b}_{10}\mathtt{x}^3+\mathtt{b}_{11}\mathtt{y}(1-\mathtt{y})-\mathtt{b}_{12}\mathtt{z}-\mathtt{b}_{13}\mathtt{z}^2-\mathtt{b}_{14}\mathtt{z}^3+\mathtt{b}_{21},\\
{}^{\mathtt{AB}}\mathscr{D}^{\rho}_{0,t}\mathtt{z} &= \mathtt{b}_{15}\mathtt{y}+\mathtt{b}_{16}\mathtt{y}^2+\mathtt{b}_{17}\mathtt{y}^3-\mathtt{b}_{18}\mathtt{z}-\mathtt{b}_{19}\mathtt{y}\mathtt{z}-d_3(\mathtt{x}(t)+\mathtt{y}(t)).
\end{aligned} \tag{2}$$

The last term in equation (2), specifically $-d_3(x(t)+y(t))$, represents a control mechanism introduced to stabilize the chaotic behavior of the glucose-insulin system. This term accounts for the external influence on the system, ensuring that fluctuations in glucose $x(t)$ and insulin $y(t)$ levels do not lead to uncontrolled chaos. The parameter d_3 regulates the strength of this control, helping to maintain system equilibrium by dynamically adjusting the response of β-cells $z(t)$ to changes in glucose and insulin concentrations. This stabilization is crucial for applications such as insulin pump therapy, where maintaining homeostasis is essential for diabetes management.

3. Preliminaries

This section provides key concepts and results related to the AB fractional derivatives. Let us denote the Sobolev space of order 1 on the interval $(x,y)\in\mathbb{R}$ as $\mathtt{S}^1(x,y) := \Big\{\varphi\in L^2(x,y) : \varphi'\in L^2(x,y), x<y\Big\}$.

Definition 1 [27] The Atangana-Baleanu-Caputo (ABC) and Atangana-Baleanu--Riemann-Liouville (ABR) fractional derivatives of order $\rho\in(0,1]$ are defined as follows:

$${}^{\mathtt{AB}}_{x}\mathscr{D}^{\rho}_{0,t}\mathtt{g}(t) = \frac{\mathtt{AB}(\rho)}{1-\rho}\int_x^t \mathscr{E}_\rho\Big(-\frac{\rho}{1-\rho}(t-s)^\rho\Big)\mathtt{g}'(s)\,ds, t>0,$$

where $\mathtt{AB}(\rho(t)) = \dfrac{\mathtt{s}(\rho(t)+1-\rho(t))}{\mathtt{s}(\rho(t))}$ with a function $\mathtt{g}\in\mathtt{S}^1(x,y)$ and

$${}^{\mathtt{AB}}\mathscr{D}^{\rho}_{0,t}\mathtt{g}(t) = \frac{\mathtt{AB}(\rho)}{1-\rho}\frac{d}{dt}\int_x^t \mathscr{E}_\rho\Big(-\frac{\rho}{1-\rho}(t-s)^\rho\Big)\mathtt{g}(s)\,ds, t>0,$$

where $\mathscr{E}_{\rho,\rho}(\cdot)$ is the generalized Mittag-Leffler function [27] and $\mathtt{AB}(\rho)$ is a normalization function with the property $\mathtt{AB}(0)=\mathtt{AB}(1)=1$. □

Definition 2 [27] The fractional integral of the AB derivative is defined as:

$${}^{\mathtt{AB}}I^{\rho}_t[\mathtt{g}(t)] = \frac{1-\rho}{\mathtt{AB}(\rho)}\mathtt{g}(t)+\frac{\rho}{\mathtt{AB}(\rho)\mathtt{s}(\rho)}\int_x^t (t-s)^{\rho-1}\mathtt{g}(s)\,ds, t>0.$$

Definition 3 Let $\rho \in (0,1]$ and $\mathscr{F} \in C([0,T],\mathbb{R}_+)$. The fractional initial value problem involving the AB derivative is formulated as follows:

$$ {}^{\mathtt{AB}}_{x}\mathscr{D}^{\rho}_{0,t}\mathtt{g}(t) = \mathscr{F}(t), t \in [0,T], \text{ with } \mathtt{g}(0) = \mathtt{g}_0, $$

which admits a unique solution given by:

$$ \mathtt{g}(t) = \mathtt{g}_0 + \frac{1-\rho}{\mathtt{AB}(\rho)}\mathscr{F}(t) + \frac{\rho}{\mathtt{AB}(\rho)\mathtt{s}(\rho)}\int_x^t (t-s)^{\rho-1}\mathscr{F}(s)\,ds. $$

4. Existence and uniqueness

The fractional integral operator of Atangana-Baleanu is used in Eq. (1):

$$ \begin{aligned} \mathtt{x}(t) - \mathtt{x}(0) &= {}^{\mathtt{AB}}I_t^{\rho}\Big[\mathscr{F}_1(t,\mathtt{x})\Big], \\ \mathtt{y}(t) - \mathtt{y}(0) &= {}^{\mathtt{AB}}I_t^{\rho}\Big[\mathscr{F}_2(t,\mathtt{y})\Big], \\ \mathtt{z}(t) - \mathtt{z}(0) &= {}^{\mathtt{AB}}I_t^{\rho}\Big[\mathscr{F}_3(t,\mathtt{z})\Big], \end{aligned} \tag{3} $$

where the kernels $\mathscr{F}_1$, $\mathscr{F}_2$, and $\mathscr{F}_3$ are defined as:

$$ \begin{aligned} \mathscr{F}_1(t,\mathtt{x}) &= -\mathtt{b}_1\mathtt{x} + \mathtt{b}_2\mathtt{x}\mathtt{y} + \mathtt{b}_3\mathtt{y}^2 + \mathtt{b}_4\mathtt{y}^3 + \mathtt{b}_5\mathtt{z} + \mathtt{b}_6\mathtt{z}^2 + \mathtt{b}_7\mathtt{z}^3 + \mathtt{b}_{20}, \\ \mathscr{F}_2(t,\mathtt{y}) &= -\mathtt{b}_8\mathtt{x}\mathtt{y} - \mathtt{b}_9\mathtt{x}^2 - \mathtt{b}_{10}\mathtt{x}^3 + \mathtt{b}_{11}\mathtt{y}(1-\mathtt{y}) - \mathtt{b}_{12}\mathtt{z} - \mathtt{b}_{13}\mathtt{z}^2 - \mathtt{b}_{14}\mathtt{z}^3 + \mathtt{b}_{21}, \\ \mathscr{F}_3(t,\mathtt{z}) &= \mathtt{b}_{15}y + \mathtt{b}_{16}\mathtt{y}^2 + \mathtt{b}_{17}\mathtt{y}^3 - \mathtt{b}_{18}\mathtt{z} - \mathtt{b}_{19}\mathtt{y}\mathtt{z}. \end{aligned} $$

From Eq. (3) to Eq. (1), we obtain the Atangana-Baleanu fractional integral:

$$ \begin{aligned} \mathtt{x}(t) - \mathtt{x}(0) &= \frac{1-\rho}{\mathtt{AB}(\rho)}\mathscr{F}_1(t,\mathtt{x}) + \frac{\rho}{\mathtt{AB}(\rho)\mathtt{s}(\rho)}\int_0^t \mathscr{F}_1(\upsilon,\mathtt{x})\,d\upsilon, \\ \mathtt{y}(t) - \mathtt{y}(0) &= \frac{1-\rho}{\mathtt{AB}(\rho)}\mathscr{F}_2(t,\mathtt{y}) + \frac{\rho}{\mathtt{AB}(\rho)\mathtt{s}(\rho)}\int_0^t \mathscr{F}_2(\upsilon,\mathtt{y})\,d\upsilon, \\ \mathtt{z}(t) - \mathtt{z}(0) &= \frac{1-\rho}{\mathtt{AB}(\rho)}\mathscr{F}_3(t,\mathtt{z}) + \frac{\rho}{\mathtt{AB}(\rho)\mathtt{s}(\rho)}\int_0^t \mathscr{F}_3(\upsilon,\mathtt{z})\,d\upsilon. \end{aligned} $$

Denote:

$$ \mathtt{s}_1 = \mathtt{b}_1 + \mathtt{b}_2\rho_3, \mathtt{s}_2 = \mathtt{b}_8\rho_1 + \mathtt{b}_{11}(1+2\rho_2), \mathtt{s}_3 = \mathtt{b}_{18} + \mathtt{b}_{19}\rho_2, \tag{4} $$

where ρ_1, ρ_2, ρ_3 are some positive constants.

Proposition 1 *Assume* $\mathtt{x}$, $\mathtt{y}$, *and* $\mathtt{z}$ *are nonnegative bounded functions, i.e.* $\|\mathtt{x}(t)\| \le \rho_1$, $\|\mathtt{y}(t)\| \le \rho_2$, $\|\mathtt{z}(t)\| \le \rho_3$, *Assume the following inequality:*

$$ 0 \le M = \max\{\mathtt{s}_1, \mathtt{s}_2, \mathtt{s}_3\} < 1. $$

The kernels $\mathscr{F}_1$, $\mathscr{F}_2$, and $\mathscr{F}_3$ satisfy the Lipschitz condition. □

PROOF The kernel $\mathscr{F}_1$ is considered. If we take $\mathtt{x}$ and $\mathtt{x}_1$ as two functions, we get:

$$\begin{aligned}\|\mathscr{F}_1(t,\mathtt{x})-\mathscr{F}_1(t,\mathtt{x}_1)\| &= \|(-\mathtt{b}_1+\mathtt{b}_2\mathtt{z}(t))(\mathtt{x}(t)-\mathtt{x}_1(t))\| \leq (\mathtt{b}_1+\mathtt{b}_2\rho_3)\|\mathtt{x}(t)-\mathtt{x}_1(t)\| \\ &= \mathtt{s}_1\|\mathtt{x}(t)-\mathtt{x}_1(t)\|.\end{aligned}$$

Similar results hold for the kernels $\mathscr{F}_2$ and $\mathscr{F}_3$ using $\{\mathtt{y},\mathtt{y}_1\}$ and $\{\mathtt{z},\mathtt{z}_1\}$, respectively:

$$\begin{aligned}\|\mathscr{F}_2(t,\mathtt{y})-\mathscr{F}_2(t,\mathtt{y}_1)\| &\leq \mathtt{s}_2\|\mathtt{y}(t)-\mathtt{y}_1(t)\|, \\ \|\mathscr{F}_3(t,\mathtt{z})-\mathscr{F}_3(t,\mathtt{z}_1)\| &\leq \mathtt{s}_3\|\mathtt{z}(t)-\mathtt{z}_1(t)\|,\end{aligned}$$

where $\mathtt{s}_1$, $\mathtt{s}_2$, and $\mathtt{s}_3$ are defined in Eq. (4). Thus, the Lipschitz conditions are satisfied for $\mathscr{F}_1$, $\mathscr{F}_2$, and $\mathscr{F}_3$, as in (3.4). Since $0 \leq M = \max\{\mathtt{s}_1,\mathtt{s}_2,\mathtt{s}_3\} < 1$, the kernels are contractions. Due to the Banach fixed-point theorem, the system is unique. ■

5. Ulam-hyers stability

Definition 4 [33] There exists a constant $C_{\mathscr{F}} > 0$ with the following property: for each *varepsilon* > 0 and for each solution $\mathscr{U}^* \in W$ satisfying the inequality.

$$\left\| {}^{\mathtt{AB}}_{a}\mathscr{D}^{\rho}_{0,t}\mathscr{U}^*(t) - \mathscr{F}\left(t,\mathscr{U}^*(t)\right)\right\| \leq \varepsilon, t \in J,$$

there exists a unique solution $\mathscr{U} \in W$ of (1) with initial condition $\mathscr{U}(0) = \mathscr{U}^*(0)$ so that

$$\left\|\mathscr{U}^*(t) - \mathscr{U}(t)\right\| \leq C_{\mathscr{F}}\varepsilon, \text{for all } t \in J,$$

$$\text{with } \mathscr{U}^*(t) := \begin{pmatrix}\mathtt{x}^*(t)\\ \mathtt{y}^*(t)\\ \mathtt{z}^*(t)\end{pmatrix}, \mathscr{U}^*(0) := \begin{pmatrix}\mathtt{x}^*(0)\\ \mathtt{y}^*(0)\\ \mathtt{z}^*(0)\end{pmatrix}, \mathscr{F}\left(t,\mathscr{U}^*(t)\right) := \begin{pmatrix}\mathscr{F}_1(t,\mathtt{x}^*)\\ \mathscr{F}_2(t,\mathtt{y}^*)\\ \mathscr{F}_3(t,\mathtt{z}^*)\end{pmatrix},$$

$$\varepsilon = \max\begin{pmatrix}\varepsilon_1\\ \varepsilon_2\\ \varepsilon_3\end{pmatrix}, C_{\mathscr{F}} := \max\begin{pmatrix}C_{\mathscr{F}_1}\\ C_{\mathscr{F}_2}\\ C_{\mathscr{F}_3}\end{pmatrix}. \qquad \square$$

This $C_{\mathscr{F}}$ is referred to as a Ulam-Hyers stability constant.

Definition 5 Whenever there is a continuous function $\Pi_{\mathscr{F}} : J \to \mathbb{R}_+$ that solves the fractional problem (1), it is said to be Ulam-Hyers stable. There exists one solution $\mathscr{U}^* \in W$ to (1), satisfying

$$\left\|\mathscr{U}^*(t) - \mathscr{U}(t)\right\| \leq \Pi_{\mathscr{F}}(\varepsilon), \text{for all } t \in J.$$

Remark 1 Considering the stability of the model, we take into account a small perturbation $\Phi(t) \in C(J)$ so that $\Phi(0) = 0$ and the following properties are satisfied:

(i) $|\Phi(t)| \leq \varepsilon$ for $t \in J$ and $\varepsilon > 0$;

(ii) ${}^{\mathtt{AB}}_{0}\mathscr{D}^{\rho}_{0,t}\mathscr{U}^{*}(t) = \mathscr{F}\Big(t,\mathscr{U}^{*}(t)\Big) + \Phi(t)$, for all $t \in J$, where $\Phi(t) = \begin{pmatrix}\Phi_1(t)\\ \Phi_2(t)\\ \Phi_3(t)\end{pmatrix}$. □

Lemma 1 *The solution $\mathscr{U}^{*}_{\Phi}(t)$ of the perturbed problem*

$$ {}^{\mathtt{AB}}_{a}\mathscr{D}^{\rho}_{0,t}\mathscr{U}^{*}(t) = \mathscr{F}\Big(t,\mathscr{U}^{*}(t)\Big) + \Phi(t), t \in J, \mathscr{U}^{*}(0) = \mathscr{U}^{*}_{0},$$

satisfies the inequality

$$\Big|\mathscr{U}^{*}_{\Phi}(t) - \mathscr{U}^{*}(t)\Big| \leq \rho\varepsilon,$$

where $\rho := \Big[\dfrac{1-\rho}{\mathtt{AB}(\rho)} + \dfrac{T^{\rho}}{\mathtt{AB}(\rho)\mathtt{s}(\rho)}\Big]$. □

PROOF We have

$$\mathscr{U}^{*}(t) = \mathscr{U}^{*}_{0} + \frac{1-\rho}{\mathtt{AB}(\rho)}\mathscr{F}\Big(t,\mathscr{U}^{*}(t)\Big) + \frac{\rho}{\mathtt{AB}(\rho)\mathtt{s}(\rho)}\int_{0}^{t}(t-s)^{\rho-1}\mathscr{F}\Big(s,\mathscr{U}^{*}(s)\Big)ds.$$

The difference between perturbed and unperturbed solutions satisfies:

$$\Big|\mathscr{U}^{*}_{\Phi}(t) - \mathscr{U}^{*}(t)\Big| \leq \frac{1-\rho}{\mathtt{AB}(\rho)}|\Phi(t)| + \frac{\rho}{\mathtt{AB}(\rho)\mathtt{s}(\rho)}\int_{0}^{t}(t-s)^{\rho-1}|\Phi(s)|ds.$$

Since it is assumed that $|\Phi(t)| \leq \varepsilon$ for all $t \in J$, substituting this bound gives:

$$\Big|\mathscr{U}^{*}_{\Phi}(t) - \mathscr{U}^{*}(t)\Big| \leq \frac{1-\rho}{\mathtt{AB}(\rho)}\varepsilon + \frac{\rho}{\mathtt{AB}(\rho)\mathtt{s}(\rho)}\int_{0}^{t}(t-s)^{\rho-1}\varepsilon\, ds.$$

The integral is computed as:

$$\int_{0}^{t}(t-s)^{\rho-1}ds = \frac{t^{\rho}}{\rho}.$$

Substituting this result:

$$\Big|\mathscr{U}^{*}_{\Phi}(t) - \mathscr{U}^{*}(t)\Big| \leq \frac{1-\rho}{\mathtt{AB}(\rho)}\varepsilon + \frac{\rho}{\mathtt{AB}(\rho)\mathtt{s}(\rho)}\cdot\frac{t^{\rho}}{\rho}\varepsilon.$$

Simplifying:

$$\Big|\mathscr{U}^{*}_{\Phi}(t) - \mathscr{U}^{*}(t)\Big| \leq \left[\frac{1-\rho}{\mathtt{AB}(\rho)} + \frac{t^{\rho}}{\mathtt{AB}(\rho)\mathtt{s}(\rho)}\right]\varepsilon.$$

Since $t \in J$ and $t^{\rho} \leq T^{\rho}$ for $t \leq T$, replacing t^{ρ} by T^{ρ} yields:

$$\Big|\mathscr{U}^{*}_{\Phi}(t) - \mathscr{U}^{*}(t)\Big| \leq \left[\frac{1-\rho}{\mathtt{AB}(\rho)} + \frac{T^{\rho}}{\mathtt{AB}(\rho)\mathtt{s}(\rho)}\right]\varepsilon.$$

Thus, the proof is complete. ■

Theorem 1 *Model (1) is Ulam-Hyers stable in W under Lemma 1 if*

$$1-\rho L_{\mathscr{F}} > 0.$$

PROOF Suppose $\mathscr{U}^* \in W$ satisfies the inequality (5), and $\mathscr{U}^*$ is the unique solution of problem (1) with the initial condition $\mathscr{U}(0) = \mathscr{U}^*(0) \Longleftrightarrow \mathscr{U}_0 = \mathscr{U}_0^*$. Then, by Lemma 1, we have

$$\mathscr{U}(t) = \mathscr{U}_0^* + \frac{1-\rho}{\mathtt{AB}(\rho)}\mathscr{F}(t,\mathscr{U}(t)) + \frac{\rho}{\mathtt{AB}(\rho)\mathtt{s}(\rho)}\int_0^t (t-s)^{\rho-1}\mathscr{F}(s,U(s))ds.$$

Thus, the proof is complete. ∎

6. Sumudu transform (ST) solution to fractional model

In fractional models of glucose-insulin regulation, obtaining an exact solution can be challenging. The ST will be applied iteratively to find an approximate solution. The ST is combined with its inverse to achieve this. The ST of the fractional derivative is given by:

$$\mathtt{S}\Big\{{}^{\mathtt{AB}}_{0}\mathscr{D}_t^{\rho}\Phi(t)\Big\} = \frac{\mathtt{AB}(\rho)}{1-\rho}\Big(\rho\mathtt{s}(\rho+1)\mathscr{E}_{\rho}\Big(-\frac{1}{1-\rho}u^{\rho}\Big)\Big)\Big[\mathtt{S}(\Phi(t)) - \Phi(0)\Big].$$

The ST and its inverse are represented in equations (1):

$$\begin{aligned}
\mathtt{x}(t) &= x(0) + \mathtt{S}^{-1}\Big\{\mathscr{L}\cdot\mathtt{S}\Big[\mathscr{F}_1(t,\mathtt{x})\Big]\Big\},\\
\mathtt{y}(t) &= y(0) + \mathtt{S}^{-1}\Big\{\mathscr{L}\cdot\mathtt{S}\Big[\mathscr{F}_2(t,\mathtt{y})\Big]\Big\},\\
\mathtt{z}(t) &= z(0) + \mathtt{S}^{-1}\Big\{\mathscr{L}\cdot\mathtt{S}\Big[\mathscr{F}_3(t,\mathtt{z})\Big]\Big\}.
\end{aligned}$$

An iterative formula is proposed as follows:

$$\begin{aligned}
\mathtt{x}_{n+1}(t) &= x(0) + \mathtt{S}^{-1}\Big\{\mathscr{L}\cdot\mathtt{S}\Big[\mathscr{F}_1(t,\mathtt{x})\Big]\Big\},\\
\mathtt{y}_{n+1}(t) &= y(0) + \mathtt{S}^{-1}\Big\{\mathscr{L}\cdot\mathtt{S}\Big[\mathscr{F}_2(t,\mathtt{y})\Big]\Big\},\\
\mathtt{z}_{n+1}(t) &= z(0) + \mathtt{S}^{-1}\Big\{\mathscr{L}\cdot\mathtt{S}\Big[\mathscr{F}_3(t,\mathtt{z})\Big]\Big\},
\end{aligned}$$

where $\mathscr{L} = \dfrac{1-\rho}{\mathtt{AB}(\rho)\rho\mathtt{s}(\rho+1)\mathscr{E}_{\rho}\Big(-\frac{1}{1-\rho}u^{\rho}\Big)}$ is the fractional Lagrange multiplier. It is assumed that the approximate solution can be obtained as the limit when $n \to \infty$: $\mathtt{x}(t) = \lim\limits_{n\to\infty}\mathtt{x}_n(t), \mathtt{y}(t) = \lim\limits_{n\to\infty}\mathtt{y}_n(t), \mathtt{z}(t) = \lim\limits_{n\to\infty}\mathtt{z}_n(t)$.

7. Atangana-Baleanu numerical scheme

We use Atangana-Baleanu derivatives with fractional order ρ as follows:

$$ {}^{\mathtt{AB}}_{0}\mathscr{D}^{\rho(t)}_{0,t}\Lambda(t) = \Phi(t,\Lambda(t)), $$

where Atangana-Baleanu derivatives are defined as weighted combinations of local fractional derivatives and nonlocal memory terms. Numerical representation: at time step t_{n+1}:

$$ \Lambda_{n+1} = \Lambda_0 + \frac{1-\rho(t)}{\mathtt{AB}(\rho(t))}\Phi(t_n,\Lambda_n) + \frac{\rho(t)}{\mathtt{AB}(\rho(t))}\sum_{\tau=0}^{n}\int_{t_\tau}^{t_{\tau+1}}\Phi(\mathtt{s},y(\mathtt{s}))(t_{n+1}-\mathtt{s})^{\rho(t)-1}\,d\mathtt{s}. $$

To approximate the integral term, we use Lagrange interpolation for the function $\Phi(\mathtt{s},y(\mathtt{s}))$. Interpolating between t_τ and $t_{\tau+1}$, we have:

$$ \Phi(\mathtt{s},y(\mathtt{s})) \approx \frac{\Phi(t_\tau,\Lambda_\tau)}{h}(\mathtt{s}-t_{\tau-1}) - \frac{\Phi(t_{\tau-1},\Lambda_{\tau-1})}{h}(\mathtt{s}-t_\tau). $$

Substituting this approximation into the integral, the numerical scheme becomes:

$$ \begin{aligned} \Lambda_{n+1} = \Lambda_0 + \frac{1-\rho(t)}{\mathtt{AB}(\rho(t))}\Phi(t_n,\Lambda_n) + \frac{\rho(t)}{\mathtt{AB}(\rho(t))}\sum_{\tau=0}^{n}\Big[\frac{\Phi(t_\tau,\Lambda_\tau)}{h}\int_{t_\tau}^{t_{\tau+1}}(\mathtt{s}-t_{\tau-1}) \\ \times(t_{n+1}-\mathtt{s})^{\rho(t)-1}\,d\mathtt{s} - \frac{\Phi(t_{\tau-1},\Lambda_{\tau-1})}{h}\int_{t_\tau}^{t_{\tau+1}}(\mathtt{s}-t_\tau)(t_{n+1}-\mathtt{s})^{\rho(t)-1}\,d\mathtt{s}\Big]. \end{aligned} $$

For a system of equations, the scheme can be extended as follows. Let $\mathscr{F}_1,\mathscr{F}_2,\mathscr{F}_3$ represent the right-hand sides of the system. Then:

$$ \begin{aligned} \mathtt{x}_{n+1} = \mathtt{x}_0 + \frac{1-\rho(t)}{\mathtt{AB}(\rho(t))}\mathscr{F}_1(t_n,\mathtt{x}_n) + \frac{\rho(t)}{\mathtt{AB}(\rho(t))}\sum_{\tau=0}^{n}\Big[\frac{\mathscr{F}_1(t_\tau,\mathtt{x}_\tau)}{h}\times\int_{t_\tau}^{t_{\tau+1}}(\mathtt{s}-t_{\tau-1}) \\ \times(t_{n+1}-\mathtt{s})^{\rho(t)-1}\,d\mathtt{s} - \frac{\mathscr{F}_1(t_{\tau-1},\mathtt{x}_{\tau-1})}{h}\times\int_{t_\tau}^{t_{\tau+1}}(\mathtt{s}-t_\tau)(t_{n+1}-\mathtt{s})^{\rho(t)-1}\,d\mathtt{s}\Big], \end{aligned} $$

with similar expressions for $\mathtt{y}_{n+1}$ and $\mathtt{z}_{n+1}$.

7.1. Numerical simulations

The numerical values are taken from Shabestari et al. [7]: $x(0)=0$, $y(0)=1.5$, and $z(0)=1$. Figures 1-2 show the comparison between the time series of system (1), illustrated in (a)-(c), and the controlled system (2), illustrated in (d)-(f), for the following cases: $\rho(t)=0.97+0.03\,cos(t/10)$, $\rho(t)=0.97+0.03\,tanh(t/10)$.

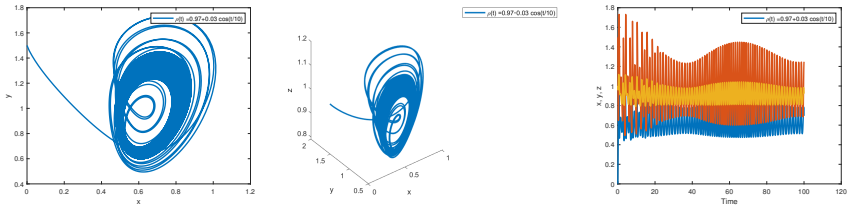

(a) xy phase plane projection (b) xyz phase plane projection (c) xyz phase plane projection

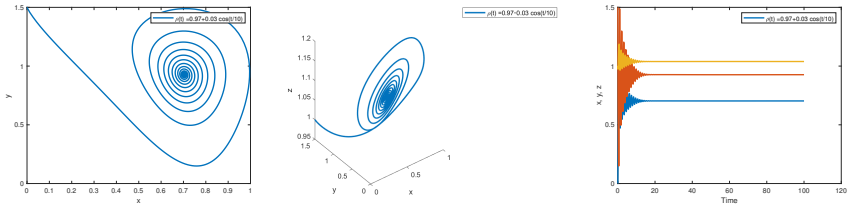

(d) xy phase plane projection (e) xyz phase plane projection (f) Time series of x, y, z

Fig. 1. Synchronization of system (1) illustrated in (a)-(c) and controlled system (2) illustrated in (d)-(f) for $\rho(t) = 0.97 + 0.03\,cos(t/10)$

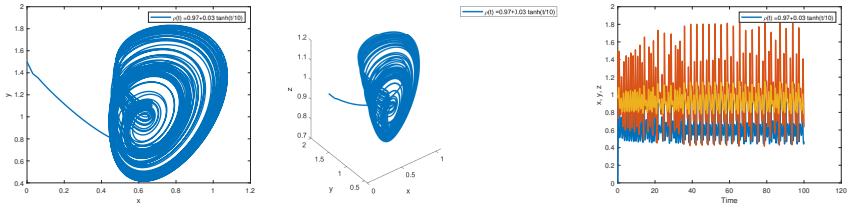

(a) xy phase plane projection (b) xyz phase plane projection (c) xyz phase plane projection

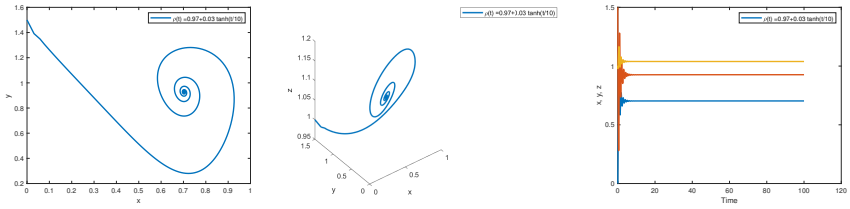

(d) xy phase plane projection (e) xyz phase plane projection (f) Time series of x, y, z

Fig. 2. Synchronization of system (1) illustrated in (a)-(c) and controlled system (2) illustrated in (d)-(f) for $\rho(t) = 0.97 + 0.03\,tanh(t/10)$

8. Conclusion

In this study, the Atangana-Baleanu fractional derivative is used to develop an advanced glucose-insulin regulatory model that incorporates long-term memory

and non-local effects. However, integer-order models fail to capture the memory--dependent dynamics of physiological systems. In glucose-insulin interactions, complex, chaotic feedback mechanisms are better represented by integrating the Atangana-Baleanu derivative. Despite the increased computational complexity, its accuracy and ability to account for long-term physiological changes justify its implementation. This model includes a linear controller, which effectively stabilizes chaotic fluctuations, enhancing its therapeutic potential in diabetes management. Several challenges remain, including accurately capturing glucose-insulin interactions, and tuning model parameters to reflect individual patient variability. However, the fractional Atangana-Baleanu derivative model enhances the flexibility of glucose--insulin dynamics modeling, making metabolic responses more precise. As a result of this refined approach to modeling, personalized treatment strategies may be developed, ultimately resulting in improved patient outcomes.

References

[1] Bagust, A., Hopkinson, P.K., Maslove, L., Currie, C.J. (2002). The projected health care burden of type 2 diabetes in the UK from 2000 to 2060. *Diabetic Medicine*, *19*(1), 1-5.

[2] Baghdadi, G., Hosseini, S.M., & Fathizadeh, A. (2015). Nonlinear dynamics of glucose-insulin interactions: An experimental study and mathematical modeling. *Journal of Theoretical Biology*, *364*, 21-30.

[3] Molnar, G.D., Taylor, W.F., & Rosevear, J.W. (1972). Day-to-day variation of continuously monitored glycaemia: A further measure of diabetic instability. *Diabetologia*, *8*(6), 342-348.

[4] Rolo, A.P., & Palmeira, C.M. (2006). Diabetes and mitochondrial function: Role of hyperglycemia and oxidative stress. *Toxicology and Applied Pharmacology*, *212*, 2, 167-178.

[5] Ackerman, E., et al. (1964). A mathematical model of the glucose-tolerance test. *Phys. Med. Biol.*, *9*(2), 203.

[6] Bajaj, M., Pintar, J., & Shoelson, S.E. (1987). Insulin action in cultured cells expressing the omega-cell line. *Journal of Biological Chemistry*, *262*(12), 5563-5566.

[7] Shabestari, M., Salimifar, R., & Rabiee, M. (2018). Chaotic behavior of glucose-insulin regulatory system using a predator-prey model. *Chaos, Solitons & Fractals*, *114*, 1-10.

[8] Holt, R.I., et al. (2017). *Textbook of Diabetes* (5th ed.). Wiley-Blackwell.

[9] Uçar, S. (2021). Existence and uniqueness results for a smoking model with determination and education in the frame of non-singular derivatives. *Discrete and Continuous Dynamical Systems-S*, *14*(7), 2571-2589.

[10] Uçar, S., Özdemir, N., Koca, İ. et al. (2020). Novel analysis of the fractional glucose-insulin regulatory system with non-singular kernel derivative. *Eur. Phys. J. Plus*, *135*, 414.

[11] Uçar, E., et al. (2021). Investigation of e-cigarette smoking model with Mittag-Leffler kernel. *Found. Comput. Decis. Sci.*, *46*, 97-109.

[12] Uçar, S., et al. (2019). Mathematical analysis and numerical simulation for a smoking model with Atangana-Baleanu derivative. *Chaos, Solitons & Fractals*, *118*, 300-306.

[13] Özdemir, N., & Uçar, E. (2020). Investigating of an immune system-cancer mathematical model with Mittag-Leffler kernel[J]. *AIMS Mathematics*, *5*(2), 1519-1531.

[14] Yadav, A.K., et al. (2022). Reflection of hygrothermal waves in a nonlocal theory of coupled thermo-elasticity. *Mechanics of Advanced Materials and Structures*, *31*(5), 1083-1096.

[15] Marin, M., Abbas, I., & Kumar, R. (2014). Relaxed Saint-Venant principle for thermoelastic micropolar diffusion. *Structural Engineering and Mechanics*, *51*, 4, 651-662.

[16] Marin, M., & Marinescu, C. (1998). Thermoelasticity of initially stressed bodies: Asymptotic equipartition of energies. *International Journal of Engineering Science*, *36*(1), 73-86.

[17] Marin, M. (2009). On the minimum principle for dipolar materials with stretch. *Nonlinear Analysis: Real World Applications*, *10*(3), 1572-1578.

[18] Abouelregal, A.E., Marin, M., & Askar, S.S. (2023). Analysis of the magneto-thermoelastic vibrations of rotating Euler-Bernoulli nanobeams using the nonlocal elasticity model. *Boundary Value Problems*, *2023*, 21.

[19] Almutairi, N., & Saber, S. (2023). Chaos control and numerical solution of time-varying fractional Newton-Leipnik system using fractional Atangana-Baleanu derivatives. *AIMS Mathematics*, *8*(11), 25863-25887.

[20] Yan, T., et al. (2024). Analysis of a Lorenz model using adomian decomposition and fractal--fractional operators. *Thermal Science*, *28*(6B), 5001-5009.

[21] Alsulami, A., et al. (2024). Controlled chaos of a fractal-fractional Newton-Leipnik system. *Thermal Science*, *28*(6B), 5153-5160.

[22] Alhazmi, M., et al. (2024). Numerical approximation method and chaos for a chaotic system in sense of Caputo-Fabrizio operator. *Thermal Science*, *28*(6B), 5161-5168.

[23] Saber, S., & Alalyani, A. (2022). Stability analysis and numerical simulations of IVGTT glucose-insulin interaction models with two time delays. *Mathematical Modelling and Analysis*, *27*, 3, 383-407.

[24] Caputo, M., & Fabrizio, M. (2015). A new definition of fractional derivative without singular kernel. *Progress in Fractional Differentiation and Applications*, *1*(2), 73-85.

[25] Elsadany, A.A. (2012). Complex dynamics in a fractional-order predator-prey model. *Nonlinear Dynamics*, *67*(4), 2281-2289.

[26] Rihan, F.A., & Hashim, S. (2016). Fractional modeling of the immune response with memory. *Mathematical Methods in the Applied Sciences*, *39*(4), 1009-1020.

[27] Atangana, A., & Baleanu, D. (2016). New fractional derivatives with non-local and non-singular kernel: Theory and application to heat transfer model. *Thermal Science*, *20*(2), 763-769.

[28] Saber, S. (2024). Control of chaos in the Burke-Shaw system of fractal-fractional order in the sense of Caputo-Fabrizio. *Journal of Applied Mathematics and Computational Mechanics*, *23*(1), 83-96.

[29] Ahmed, K., et al. (2024). Analytical solutions for a class of variable-order fractional Liu system under time-dependent variable coefficients. *Results in Physics*, *56*, 107311.

[30] Almutairi, N., & Saber, S. (2024). Existence of chaos and the approximate solution of the Lorenz-Lü-Chen system with the Caputo fractional operator. *AIP Advances*, *14*(1), 015112.

[31] Atangana, A. (2017). Fractal-fractional differentiation and integration: connecting fractal calculus and fractional calculus to predict complex systems. *Chaos Solitons Fractals*, *102*, 396-406.

[32] Rajagopal, K., & Karthikeyan, A. (2017). Chaos in fractional-order systems with biomedical applications. *Chaos: An Interdisciplinary Journal of Nonlinear Science*, *27*(6), 063118.

[33] Ulam, S.M. (1960). *A Collection of Mathematical Problems*. Interscience Publ., New York.